Nonlinear Dyn (2010) 61: 109–121
DOI 10.1007/s11071-009-9635-4

ORIGINAL PAPER

Vibration reduction of multi-parametric excited spring pendulum via a transversally tuned absorber

M. Eissa · M. Kamel · A.T. El-Sayed

Received: 7 January 2009 / Accepted: 30 November 2009 / Published online: 17 December 2009

Abstract The use of passive control strategy is a common way to stabilize and control dangerous vibrations in a nonlinear spring pendulum which is describing the ship's roll motion. In this paper, a tuned absorber in the transversal direction is connected to a spring pendulum with multi-parametric excitation forces to control the vibration due to some resonance cases on the system. The method of multiple scale perturbation technique (MSPT) is applied to study the periodic solution of the given system near simultaneous sub-harmonic and internal resonance case. The stability of the steady-state solution near the resonance case is investigated and studied using frequency response equations. The effects of the absorber and some system parameters on the vibrating system are studied numerically. Optimal working conditions of the system are extracted when applying passive control methods. Comparison with the available published work is reported.

Keywords Nonlinearity · Passive control · Stability · Pitch and roll motion

M. Eissa · M. Kamel
Department of Engineering Mathematics, Faculty of Electronic Engineering Menouf, Menoufia University, Menouf 32952, Egypt

A.T. El-Sayed (✉)
Department of Basic Sciences, Modern Academy for Engineering and Technology, Maadi, Egypt
e-mail: ashraftaha211@yahoo.com

Nomenclature

c_j $(j = 1, 2, 3, 4)$	the damping coefficient of the spring pendulum modes and the absorber $(c_j = \varepsilon \hat{c}_j)$
ω_1, ω_2 and ω_3	the natural frequency of the spring pendulum modes and absorber
α, β	the nonlinear parameters $(\beta_1 = \varepsilon \hat{\beta}_1)$
f_j	the forcing amplitude of the main system $(f_j = \varepsilon^2 \hat{f}_j)$
Ω_j	the frequencies of the main system
ε	a small perturbation parameter
g	the gravity acceleration
M, m	the masses of the spring pendulum and absorber, respectively
l	statically stretched length of the pendulum
l_1	statically stretched length of the absorber
$x, \bar{x}$	the longitudinal response of the spring pendulum $(x = \bar{x}/l)$
$u, \bar{u}$	the longitudinal response of the absorber $(u = \bar{u}/l)$
φ	the angular response of the pendulum
k_1, k_2	the linear stiffness of the spring pendulum and the absorber
k_i $(i = 3, 4, 5, 6)$	the spring stiffness of nonlinear parameters
$M(t)$	a moment acts at the point O

$F(t)$	a force acts on mass M in the x direction

1 Introduction

Vibration may cause discomfort, disturbance, damage and sometimes destruction of the system or the structure. This problem makes the vibration an undesirable phenomenon in our life, so it must be reduced or controlled or eliminated. One of the most common methods of passive vibration control is the dynamic absorber which can be added to the most engineering vibrating systems [1, 2]. The spring–pendulum system is one of the famous dynamical systems simulating many engineering applications and one of these applications is the ship's roll motion [3–5]. Lee et al. [5–7] studied harmonically excited spring–pendulum system with internal resonance applying MSPT. From this study they obtained a complex behavior jump phenomena, Hopf bifurcations and a sequence of periodic-doubling bifurcations leading to chaotic motion. Also, they observed that the second-order approximation gives better agreement with the main system than the first-order approximation does. Eissa [9] reported that one of the most effective tools for the control of passive vibration is the dynamic absorber or the damper or the neutralizer. Vibration and dynamic chaos of both simple pendulum and spring pendulum that represent ship's roll motion have been studied by Eissa and Sayed [10–14]. The effects of the transverse and longitudinal tuned absorbers on the vibrations of both systems under single harmonic excitation have been studied numerically to control the oscillations of both systems. The stability of both simple pendulum and spring pendulum near the simultaneous primary resonance conditions is studied also using frequency response equations. Zafer et al. [15] show that the parametrical numerical simulations were carried out in very steep regular waves to assess the possible improvements of a state-of-the-art numerical model of the control and capsizing behavior of ships in following and quartering seas. Lee et al. [16] analyzed the motion of a damaged ship in waves resulting from a theoretical and experimental study. The quantitative agreement between the experimental and theoretical results was found to be not so good for the roll motion. This fact can be attributed to experimental inaccuracies, particularly those related to the scaling of the water ingress and the associated viscous effects, and to the limitations of the theoretical model, especially the incomplete calibration of the water ingress phenomenon. Bayly and Virgin [17] studied experimentally the stability of periodic motion in forced spring pendulum based on analytical solutions and Floquet theory. Poincaré sampling is used to reduce the problem of describing the stability of a limit cycle to the easier task of defining the stability of the fixed point of a Poincaré map. Empirical estimates of characteristic multipliers in four-dimensional state space are obtained by examining transient behavior after perturbations; the Karhunen–Loeve decomposition is used to identify dominant local modes in these transients. Kamel [18] and Zhou and Chen [19] investigated the response and stability of two modes of ship model under sinusoidal harmonic excitation. They obtained the bifurcation response equation near the combination resonance case in the presence of internal resonance of this system. Song et al. [20] investigated the vibration response of the spring–mass–damper system with a parametrically excited pendulum hinged to the mass applying the harmonic balance method. Also, they showed that the area of unstable motion of this system obtained from the third-order approximations is to be fairly consistent with that obtained from numerical calculation. Amer and Bek [21] investigated the chaotic response of a harmonically excited spring pendulum that is moving in a circular path. The approximate system is shown to have bifurcation leading to chaos. Alasty and Shabani [22] studied the response of a spring–pendulum system. By constructing the bifurcation diagram and the Poincaré map, the chaotic and quasi-periodic motions are studied for a narrow bound of system parameters. Vyas and Bajaj [23] described the dynamics of an $(n + 1)$-degree-of-freedom auto-parametric vibration absorber which consists of an array of n pendulums. A first-order asymptotic analysis of the system has been carried out under resonant excitation conditions with 1:1:2 internal resonances. The averaged equations are used to obtain steady-state solutions of the system. Osama et al. [24] reported how the ship roll can be controlled by using active and passive control.

The work in [25] introduced the vibration and stability of the nonlinear spring pendulum describing the ship's roll motion. The obtained results illustrated the effects of the longitudinal absorber on the system under multi-parametric excitations.

The main task of the present paper is to show the effect of the control device on the angular response

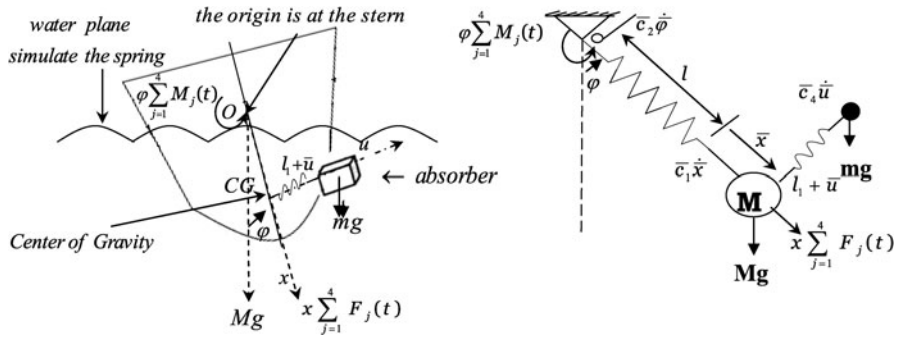

Fig. 1 Diagrammatic representation of the system

(φ) of the nonlinear spring pendulum, modifying the model in [8, 25] by connecting the spring pendulum to the transverse absorber. This leads to a three-degree-of-freedom system under multi-parametric excitations. MSPT is applied throughout to get an approximate solution up to the second-order approximations. The stability of the system is investigated near the simultaneous resonance cases applying frequency response functions. Some recommendations regarding the different parameters of the system are reported. The effects of the absorbers on system behavior are given numerically. Comparison with the available published works is reported.

2 Mathematical analysis

The diagrammatic sketch of the considered system is shown in Fig. 1. The absorber mass can move transversally in the direction perpendicular to the pendulum axis. The whole motion is the planer motion. Here φ is the angular displacement of the pendulum which is assumed small (less than 5°, because if it is large, it will cause the capsize of the ship) and x, u are the extensions of the spring and absorber, respectively, from its equilibrium position.

For convenience, we refer to the existing works [8, 14, 23, 25] on multi-parametric excited spring–pendulum system with transverse absorber in Fig. 1 for the equations of motions for the normal coordinates as follows:

$$\begin{aligned}&\ddot{x}+\varepsilon\hat{c}_1\dot{x}+\omega_1^2x+\alpha_1x^2+\alpha_2x^3\\&\quad-(1+x)\dot{\varphi}^2+\omega_2^2(1-\cos\varphi)\\&=\varepsilon^2x\sum_{j=1}^{4}\hat{f}_{1j}\cos(\Omega_{1j}T_0),\end{aligned}\tag{1}$$

$$\begin{aligned}&(1+x)^2\ddot{\varphi}+\varepsilon\hat{c}_2\dot{\varphi}+2(1+x)\dot{x}\dot{\varphi}+\omega_2^2(1+x)\sin\varphi\\&\quad+\varepsilon\hat{c}_3\big[(1+x)\dot{\varphi}-\dot{u}\big](1+x)\\&\quad+\varepsilon\hat{\beta}_1\big[(1+x)\varphi-u\big](1+x)\\&\quad+\beta_2\big[(1+x)\varphi-u\big]^2(1+x)\\&\quad+\beta_3\big[(1+x)\varphi-u\big]^3(1+x)\\&=\varepsilon^2\varphi\sum_{j=1}^{4}\hat{f}_{2j}\cos(\Omega_{2j}T_0),\end{aligned}\tag{2}$$

$$\begin{aligned}&\ddot{u}+\omega_2^2\sin\varphi+\varepsilon\hat{c}_4\big[\dot{u}-(1+x)\dot{\varphi}\big]\\&\quad+\omega_3^2\big[u-(1+x)\varphi\big]+\beta_4\big[u-(1+x)\varphi\big]^2\\&\quad+\beta_5\big[u-(1+x)\varphi\big]^3=0,\end{aligned}\tag{3}$$

where:

$$\begin{aligned}&c_1=\frac{\bar{c}_1}{M},\quad c_2=\frac{\bar{c}_2}{Ml^2},\quad c_3=\frac{\bar{c}_3}{M},\quad c_4=\frac{\bar{c}_3}{m},\\&\omega_1^2=\frac{k_1}{M},\quad \omega_2^2=\frac{g}{l},\quad \omega_3^2=\frac{k_4}{m},\quad \alpha_1=\frac{k_2l}{M},\\&\alpha_2=\frac{k_3l^2}{M},\quad \beta_1=\frac{k_4}{M},\quad \beta_2=\frac{k_5l}{M},\quad \beta_3=\frac{k_6l^2}{M},\\&\beta_4=\frac{k_5l}{m},\quad \beta_5=\frac{k_6l^2}{m},\quad f_{1j}=\frac{F_j(t)}{Ml},\\&f_{2j}=\frac{M_j(t)}{Ml^2}.\end{aligned}$$

The standard method of perturbation (MSPT) [26] is used to obtain a uniformly valid, asymptotic expansion of the solutions for (1)–(3), taking into account the resonance condition $\Omega_{12}\cong 2\omega_1$, $\Omega_{21}\cong 2\omega_2$ and $\omega_2\cong 2\omega_3$, introducing the detuning parameters σ_1, σ_2

and $\sigma_3(\sigma_n = \varepsilon\hat{\sigma}_n)$ according to

$$\Omega_{12} = 2\omega_1 + \varepsilon\hat{\sigma}_1, \quad \Omega_{21} = 2\omega_2 + \varepsilon\hat{\sigma}_2 \quad \text{and} \quad \omega_2 = 2\omega_3 + \varepsilon\hat{\sigma}_3. \tag{4}$$

The asymptotic approximate solution of (1)–(3) is in the form:

$$x(t;\varepsilon) = \sum_{n=1}^{3} \varepsilon^n x_n(T_0, T_1, T_2) + O\left(\varepsilon^4\right), \tag{5}$$

$$\varphi(t;\varepsilon) = \sum_{n=1}^{3} \varepsilon^n \varphi_n(T_0, T_1, T_2) + O\left(\varepsilon^4\right), \tag{6}$$

$$u(t;\varepsilon) = \sum_{n=1}^{3} \varepsilon^n u_n(T_0, T_1, T_2) + O\left(\varepsilon^4\right). \tag{7}$$

The derivatives will be in the form

$$\frac{d}{dt} = D_0 + \varepsilon D_1 + \varepsilon^2 D_2 \quad \text{and} \quad \frac{d^2}{dt^2} = D_0^2 + 2\varepsilon D_0 D_1 + \varepsilon^2\left(D_1^2 + 2D_0 D_2\right) \tag{8}$$

For the second-order approximation, we introduce three timescales, where $T_m = \varepsilon^m t$ and $D_m = \frac{\partial}{\partial T_m}$ $(m = 0, 1, 2)$.

Substituting (5)–(8) into (1)–(3) and equating the coefficients of equal powers of (ε) leads to

$O(\varepsilon)$:

$$\left(D_0^2 + \omega_1^2\right)x_1 = 0, \tag{9a}$$

$$\left(D_0^2 + \omega_2^2\right)\varphi_1 = 0, \tag{9b}$$

$$\left(D_0^2 + \omega_3^2\right)u_1 = \left(\omega_3^2 - \omega_2^2\right)\varphi_1; \tag{9c}$$

$O(\varepsilon^2)$:

$$\left(D_0^2 + \omega_1^2\right)x_2 = -2D_0D_1x_1 - \hat{c}_1D_0x_1 - \alpha_1x_1^2 + (D_0\varphi_1)^2 - \omega_2^2\frac{\varphi_1^2}{2}, \tag{10a}$$

$$\left(D_0^2 + \omega_2^2\right)\varphi_2 = -2D_0D_1\varphi_1 - 2x_1D_0^2\varphi_1 - \hat{c}_2D_0\varphi_1 - 2D_0x_1D_0\varphi_1 - \omega_2^2x_1\varphi_1 - \hat{c}_3(D_0\varphi_1 - D_0u_1) - \hat{\beta}_1(\varphi_1 - u_1) - \beta_2\left(u_1^2 - 2\varphi_1u_1 + \varphi_1^2\right), \tag{10b}$$

$$\left(D_0^2 + \omega_3^2\right)u_2 = -2D_0D_1u_1 - \omega_2^2\varphi_2 + \omega_3^2(x_1\varphi_1 + \varphi_2) - \hat{c}_4(D_0u_1 - D_0\varphi_1) - \beta_4\left(u_1^2 - 2\varphi_1u_1 + \varphi_1^2\right); \tag{10c}$$

$O(\varepsilon^3)$:

$$\left(D_0^2 + \omega_1^2\right)x_3 = -2D_0D_1x_2 - \left(D_1^2 + 2D_0D_2\right)x_1 - \hat{c}_1(D_0x_2 + D_1x_1) - 2\alpha_1x_1x_2 - \alpha_2x_1^3 + 2D_0\varphi_1D_0\varphi_2 + 2D_0\varphi_1D_1\varphi_1 + x_1(D_0\varphi_1)^2 - \omega_2^2\varphi_1\varphi_2 + x_1\sum_{j=1}^{4}\hat{f}_{1j}\cos(\Omega_{1j}T_0), \tag{11a}$$

$$\left(D_0^2 + \omega_2^2\right)\varphi_3 = -2D_0D_1\varphi_2 - 4x_1D_0D_1\varphi_1 - \left(D_1^2 + 2D_0D_2\right)\varphi_1 - x_1^2D_0^2\varphi_1 - 2x_2D_0^2\varphi_1 - 2x_1D_0^2\varphi_2 - \hat{c}_2(D_0\varphi_2 + D_1\varphi_1) - 2D_0x_1D_0\varphi_2 - 2D_0x_1D_1\varphi_1 - 2D_1x_1D_0\varphi_1 - 2D_0x_2D_0\varphi_1 - 2x_1D_0x_1D_0\varphi_1 - \omega_2^2x_2\varphi_1 + \frac{\omega_2^2\varphi_1^3}{6} - \omega_2^2x_1\varphi_2 - \hat{c}_3(D_1\varphi_1 - D_0u_2 + D_0\varphi_2 + 2x_1D_0\varphi_1 - D_1u_1 - x_1D_0u_1) - \hat{\beta}_1(-u_1x_1 - u_2 + 2x_1\varphi_1 + \varphi_2) - \beta_2\left(-2\varphi_1u_2 - 4x_1\varphi_1u_1 + 3\varphi_1^2x_1 + 2\varphi_1\varphi_2 - 2\varphi_2u_1 + u_1^2x_1 + 2u_1u_2\right) - \beta_3\left(-u_1^3 + 3\varphi_1u_1^2 - 3\varphi_1^2u_1 + \varphi_1^3\right) + \varphi_1\sum_{j=1}^{4}\hat{f}_{2j}\cos(\Omega_{2j}T_0), \tag{11b}$$

$$\left(D_0^2 + \omega_3^2\right)u_3 = -2D_0D_1u_2 - \left(D_1^2 + 2D_0D_2\right)u_1 - \left(\omega_2^2\varphi_3 - \frac{\omega_2^2\varphi_1^3}{6}\right) + \omega_3^2(\varphi_3 + x_1\varphi_2 + x_2\varphi_1) - \hat{c}_4(D_1u_1 - D_1\varphi_1 + D_0u_2$$

$$
\begin{aligned}
&- D_0\varphi_2 - x_1 D_0\varphi_1)\\
&- \beta_4\big(-2\varphi_1 u_2 + 2u_1 u_2 + 2\varphi_1^2 x_1\\
&- 2\varphi_2 u_1 - 2x_1\varphi_1 u_1 + 2\varphi_1\varphi_2\big)\\
&- \beta_5\big(u_1^3 - 3\varphi_1 u_1^2 + 3\varphi_1^2 u_1 - \varphi_1^3\big).
\end{aligned}
\tag{11c}
$$

The general solutions of (9) can be written in the form

$$x_1 = A_1(T_1, T_2)\exp(i\omega_1 T_0) + \text{cc.}, \tag{12a}$$

$$\varphi_1 = A_2(T_1, T_2)\exp(i\omega_2 T_0) + \text{cc.}, \tag{12b}$$

$$
\begin{aligned}
u_1 = {} & A_3(T_1, T_2)\exp(i\omega_3 T_0)\\
& + A_2(T_1, T_2)\exp(i\omega_2 T_0) + \text{cc.},
\end{aligned}
\tag{12c}
$$

where A_n are complex function in T_1 and T_2, cc. represents the complex conjugate of the previous terms.

Substituting (12) into (10) and using the response condition equation (4) leads to secular terms. Eliminating these secular terms leads to solvability for the first-order approximation:

$$2i\omega_1 D_1 A_1 = -\hat{c}_1 i\omega_1 A_1, \tag{13a}$$

$$
\begin{aligned}
2i\omega_2 D_1 A_2 = {} & -\hat{c}_2 i\omega_2 A_2\\
& + \big[-\beta_2 A_3^2\big]\exp\big(-i\hat{\sigma}_3 T_1\big),
\end{aligned}
\tag{13b}
$$

$$2i\omega_3 D_1 A_3 = \big[-\hat{c}_4 i\omega_3 A_3 - \hat{c}_3(i\omega_3 A_3) - \hat{\beta}_1 A_3\big]. \tag{13c}$$

After eliminating the secular terms, the particular solutions of (10) will be in the form:

$$
\begin{aligned}
x_2 = {} & \frac{[\alpha_1 A_1^2]}{3\omega_1^2}\exp(2i\omega_1 T_0) - \left[\frac{3\omega_2^2}{2(\omega_1^2 - 4\omega_2^2)}A_2^2\right]\\
& \times \exp(2i\omega_2 T_0) + \frac{[\omega_2^2 A_2\bar{A}_2 - 2\alpha_1 A_1\bar{A}_1]}{2\omega_1^2} + \text{cc.},
\end{aligned}
\tag{14a}
$$

$$
\begin{aligned}
\varphi_2 = {} & \frac{[\omega_2^2 A_1 A_2 + 2\omega_1\omega_2 A_1 A_2]}{\omega_2^2 - (\omega_1 + \omega_2)^2}\exp\big(i(\omega_1 + \omega_2)T_0\big)\\
& + \frac{[\omega_2^2 A_1\bar{A}_2 - 2\omega_1\omega_2 A_1\bar{A}_2]}{\omega_2^2 - (\omega_1 - \omega_2)^2}\exp\big(i(\omega_1 - \omega_2)T_0\big)\\
& + \frac{[\hat{c}_3(i\omega_3 A_3) + \hat{\beta}_1 A_3]}{\omega_2^2 - \omega_3^2}\exp(i\omega_3 T_0)\\
& - \frac{\beta_2 A_3\bar{A}_3}{\omega_2^2} + \text{cc.},
\end{aligned}
\tag{14b}
$$

$$
\begin{aligned}
u_2 = {} & \frac{[\beta_4 A_3^2]}{3\omega_3^2}\exp(2i\omega_3 T_0)\\
& + \left[\frac{(\omega_3^2 - \omega_2^2)(\omega_2^2 A_1 A_2 + 2\omega_1\omega_2 A_1 A_2)}{[\omega_3^2 - (\omega_1 + \omega_2)^2]^2}\right.\\
& \left. + \frac{\omega_3^2 A_1 A_2}{\omega_3^2 - (\omega_1 + \omega_2)^2}\right]\exp\big(i(\omega_1 + \omega_2)T_0\big)\\
& - \frac{[2i\omega_2 D_1 A_2]}{\omega_3^2 - \omega_2^2}\exp(i\omega_2 T_0)\\
& + \left[\frac{(\omega_3^2 - \omega_2^2)(\omega_2^2 A_1\bar{A}_2 - 2\omega_1\omega_2 A_1\bar{A}_2)}{[\omega_3^2 - (\omega_1 - \omega_2)^2]^2}\right.\\
& \left. + \frac{\omega_3^2 A_1\bar{A}_2}{\omega_3^2 - (\omega_1 - \omega_2)^2}\right]\exp\big(i(\omega_1 - \omega_2)T_0\big)\\
& + \frac{[-(\omega_3^2 - \omega_2^2)\frac{\beta_2 A_3\bar{A}_3}{\omega_2^2} - \beta_4 A_3\bar{A}_3]}{\omega_3^2} + \text{cc.}
\end{aligned}
\tag{14c}
$$

Substituting (12), (14) into (11) and using the response condition equation (4) leads to secular terms. Eliminating these secular terms leads to solvability for the second-order approximation:

$$
\begin{aligned}
2i\omega_1 D_2 A_1 = {} & \big[-D_1^2 A_1 - \hat{c}_1 D_1 A_1\\
& + \eta_1 A_1 A_2\bar{A}_2 + \eta_2 A_1^2\bar{A}_1\big]\\
& + \left[\frac{\hat{f}_{12}}{2}\bar{A}_1\right]\exp\big(i\hat{\sigma}_1 T_1\big),
\end{aligned}
\tag{15a}
$$

$$
\begin{aligned}
2i\omega_2 D_2 A_2 = {} & \big[\eta_4 D_1 A_2 - D_1^2 A_2 + \eta_1 A_1\bar{A}_1 A_2\\
& + \eta_3 A_2^2\bar{A}_2\big] + \big[\eta_5 A_3^2\big]\exp\big(-i\hat{\sigma}_3 T_1\big)\\
& + \left[\frac{\hat{f}_{21}}{2}\bar{A}_2\right]\exp\big(i\hat{\sigma}_2 T_1\big),
\end{aligned}
\tag{15b}
$$

$$
\begin{aligned}
2i\omega_3 D_2 A_3 = {} & -D_1^2 A_3 + \eta_6 D_1 A_3 + \eta_7 A_3^2\bar{A}_3 + \eta_8 A_3\\
& + \big[4\eta_9\bar{A}_3 i\omega_2 D_1 A_2\big]\exp\big(i\hat{\sigma}_3 T_1\big),
\end{aligned}
\tag{15c}
$$

where η_s $\{s = 1, 2, \ldots, 9\}$ are constants (see Appendix).

3 Periodic solution

The simultaneous sub-harmonic and internal resonance case ($\Omega_{12} \cong 2\omega_1$, $\Omega_{21} \cong 2\omega_2$, $\omega_2 \cong 2\omega_3$), which is the worst resonance case, has been chosen to study the stability from the second-order approximation solution.

From the first part of (8), multiplying both sides by $2i\omega_n$ can express the derivative of A_n with respect to t:

$$2i\omega_n \frac{dA_n}{dt} = \varepsilon 2i\omega_n D_1 A_n + \varepsilon^2 2i\omega_n D_2 A_n + O(\varepsilon^3). \tag{16}$$

To analyze the solution of (13), (15), it is convenient to express $A_n(T_1, T_2)$ in the form

$$A_n = \left(\frac{\hat{a}_n}{2}\right)\exp(i\gamma_n), \quad a_n = \varepsilon\hat{a}_n, \tag{17}$$

where a_n and γ_n are real and represent the steady-state amplitudes and the phases of the motions, respectively. Inserting (17) and (13), (15) into (16) and equating the real and imaginary parts, the following equations are obtained:

$$\dot{a}_1 = -\frac{c_1}{2}a_1 + \frac{f_{12}}{4\omega_1}a_1\sin(\theta_1), \tag{18a}$$

$$a_1\dot{\gamma}_1 = -\frac{c_1^2}{8\omega_1}a_1 - \frac{\eta_1}{8\omega_1}a_1a_2^2 - \frac{\eta_2}{8\omega_1}a_1^3 - \frac{f_{12}}{4\omega_1}a_1\cos(\theta_1), \tag{18b}$$

$$\dot{a}_2 = -\frac{c_2}{2}a_2 + \left(\frac{c_2\beta_1}{2(\omega_3^2-\omega_2^2)}\right)a_2 + \frac{f_{21}}{4\omega_2}a_2\sin(\theta_2) + \eta_{10}\frac{a_3^2}{4}\sin(\theta_3) + \eta_{11}\frac{a_3^2}{4}\cos(\theta_3), \tag{19a}$$

$$a_2\dot{\gamma}_2 = \eta_{12}a_2 - \frac{\eta_1}{8\omega_2}a_1^2a_2 - \frac{\eta_3}{8\omega_2}a_2^3 - \frac{f_{21}}{4\omega_2}a_2\cos(\theta_2) + \eta_{10}\frac{a_3^2}{4}\cos(\theta_3) - \eta_{11}\frac{a_3^2}{4}\sin(\theta_3), \tag{19b}$$

$$\dot{a}_3 = \left[\frac{c_2\beta_1}{2(\omega_2^2-\omega_3^2)} - \frac{c_4}{2} - \frac{c_3}{2}\right]a_3 - c_2\eta_9\frac{\omega_2a_2a_3}{2\omega_3}\cos(\theta_3), \tag{20a}$$

$$a_3\dot{\gamma}_3 = \eta_{13}a_3 + [-\eta_7 + 2\eta_9\beta_2]\frac{a_3^3}{8\omega_3} - c_2\eta_9\frac{\omega_2a_2a_3}{2\omega_3}\sin(\theta_3), \tag{20b}$$

where $\theta_1 = \hat{\sigma}_1T_1 - 2\gamma_1$, $\theta_2 = \hat{\sigma}_2T_1 - 2\gamma_2$, $\theta_3 = \hat{\sigma}_3T_1 + \gamma_2 - 2\gamma_3$ and $\eta_k\{k = 10, 11, 12, 13\}$ are constants (see Appendix).

Thus, the first approximation periodic solution can be written in the form

$$x_1 = a_1\cos\left[\frac{1}{2}(\Omega_{12}T_0 - \theta_1)\right], \tag{21a}$$

$$\varphi_1 = a_2\cos\left[\frac{1}{2}(\Omega_{21}T_0 - \theta_2)\right], \tag{21b}$$

$$u_1 = a_3\cos\left[\frac{1}{4}\big(\Omega_{21}T_0 - (\theta_2 + 2\theta_3)\big)\right] + a_2\cos\left[\frac{1}{2}(\Omega_{21}T_0 - \theta_2)\right], \tag{21c}$$

where a_1, a_2, a_3, θ_1, θ_2 and θ_3 are obtained by the solutions of (18)–(20).

3.1 Stability of the fixed points

The steady-state solution of our dynamical system corresponding to the fixed point of (18)–(20) is obtained when $\dot{a}_n = 0$ and $\dot{\theta}_n = 0$; then we can get the frequency response equations (FRE) for practical case ($a_1 \neq 0, a_2 \neq 0, a_3 \neq 0$) as follows:

$$\sigma_1^2 + \left(\frac{\eta_1}{2\omega_1}a_2^2 + \frac{\eta_2}{2\omega_1}a_1^2 + \frac{1}{2\omega_1}c_1^2\right)\sigma_1 + c_1^2 + \frac{1}{16\omega_1^2}\left[(\eta_1a_2^2 + \eta_2a_1^2) + c_1^2\right]^2 - \frac{f_{12}^2}{4\omega_1^2} = 0, \tag{22a}$$

$$\sigma_2^2 + \left(\frac{\eta_1}{2\omega_2}a_1^2 + \frac{\eta_3}{2\omega_2}a_2^2 - 4\eta_{12}\right)\sigma_2 + 4\left(-\eta_{12} + \frac{\eta_1}{8\omega_2}a_1^2 + \frac{\eta_3}{8\omega_2}a_2^2\right)^2 + \left(c_2 - \frac{c_2\beta_1}{(\omega_3^2-\omega_2^2)}\right)^2 - \frac{f_{21}^2}{4\omega_2^2} - \left(\frac{\eta_{10}^2}{4} + \frac{\eta_{11}^2}{4}\right)\frac{a_3^4}{a_2^2} + \frac{f_{21}}{2a_2\omega_2}\eta_{10}a_3^2\cos(\theta_2 + \theta_3) - \frac{f_{21}}{2a_2\omega_2}\eta_{11}a_3^2\sin(\theta_2 + \theta_3) = 0, \tag{22b}$$

$$\sigma_3^2 + \left[-4\eta_{13} - (-\eta_7 + 2\eta_9\beta_2)\frac{a_3^2}{2\omega_3} + \sigma_2\right]\sigma_3 + \left[-\sigma_2 + 4\eta_{13} + (-\eta_7 + 2\eta_9\beta_2)\frac{a_3^2}{2\omega_3}\right] + \left[\frac{c_2\beta_1}{(\omega_2^2-\omega_3^2)} - c_4 - c_3\right]^2 - \frac{\omega_2^2c_2^2\eta_9^2a_2^2}{\omega_3^2} = 0. \tag{22c}$$

To determine the stability of the steady-state solution, one lets

$$a_n = a_{n0} + a_{n1}, \qquad \theta_n = \theta_{n0} + \theta_{n1}, \tag{23}$$

where a_{n0} and θ_{n0} are the solutions of (18)–(20) and a_{n1}, θ_{n1} are perturbations which are assumed to be small compared with a_{n0} and θ_{n0}. Substituting (23) into (18)–(20) and keeping only the linear terms in a_{n1} and θ_{n1}, we obtain

$$\dot{a}_{11} = \left[-\frac{c_1}{2} + \frac{f_{12}}{4\omega_1}\sin(\theta_{10})\right]a_{11} + \left[\frac{f_{12}}{4\omega_1}a_{10}\cos(\theta_{10})\right]\theta_{11}, \tag{24a}$$

$$\dot{\theta}_{11} = \left[\frac{\sigma_1}{a_{10}} + \frac{c_1^2}{4\omega_1 a_{10}} + \frac{\eta_1 a_{20}^2}{4\omega_1 a_{10}} + \frac{3a_{10}\eta_2}{4\omega_1} + \frac{f_{12}}{2\omega_1 a_{10}}\cos(\theta_{10})\right]a_{11} + \left[\frac{\eta_1 a_{20}}{2\omega_1}\right]a_{21} - \left[\frac{f_{12}}{2\omega_1}\sin(\theta_{10})\right]\theta_{11}, \tag{24b}$$

$$\dot{a}_{21} = \left[-\frac{c_2}{2} + \left(\frac{c_2\beta_1}{2(\omega_3^2-\omega_2^2)}\right) + \frac{f_{21}}{4\omega_2}\sin(\theta_{20})\right]a_{21} + \left[\frac{f_{21}}{4\omega_2}a_{20}\cos(\theta_{20})\right]\theta_{21} + \left[\frac{3\eta_{10}a_{30}^2}{4}\sin(\theta_{30}) + \frac{\eta_{11}a_{30}}{2}\cos(\theta_{30})\right]a_{31} + \left[\frac{\eta_{10}a_{30}^3}{4}\cos(\theta_{30}) - \frac{\eta_{11}a_{30}^2}{4}\sin(\theta_{30})\right]\theta_{31}, \tag{25a}$$

$$\dot{\theta}_{21} = \left[\frac{\sigma_2}{a_{20}} - \frac{2\eta_{12}}{a_{20}} + \frac{\eta_1 a_{10}^2}{4\omega_2 a_{20}} + \frac{3a_{20}\eta_3}{4\omega_2} + \frac{f_{21}}{2a_{20}\omega_2}\cos(\theta_{20})\right]a_{21} + \left[\frac{\eta_1}{2\omega_2}a_{10}\right]a_{11} - \left[\frac{f_{21}}{2\omega_2}\sin(\theta_{20})\right]\theta_{21} + \left[\frac{-a_{30}\eta_{10}}{a_{20}}\cos(\theta_{30}) + \frac{a_{30}\eta_{11}}{a_{20}}\sin(\theta_{30})\right]a_{31} + \left[\frac{\eta_{10}a_{30}^2}{2a_{20}}\sin(\theta_{30}) + \frac{\eta_{11}a_{30}^2}{2a_{20}}\cos(\theta_{30})\right]\theta_{31} \tag{25b}$$

$$\dot{a}_{31} = \left[\frac{c_2\beta_1}{2(\omega_2^2-\omega_3^2)} - \frac{c_4}{2} - \frac{c_3}{2} - \frac{c_2\eta_9\omega_2 a_{20}}{2\omega_3} \times \cos(\theta_{30})\right]a_{31} + \left[\frac{c_2\eta_9\omega_2 a_{20}a_{30}}{2\omega_3}\sin(\theta_{30})\right]\theta_{31} - \left[\frac{c_2\eta_9\omega_2 a_{30}}{2\omega_3}\cos(\theta_{30})\right]a_{21}, \tag{26a}$$

$$\dot{\theta}_{31} = \left[\frac{2\sigma_3+\sigma_2}{a_{30}} - \frac{4\eta_{13}}{a_{30}} - (-\eta_7+2\eta_9\beta_2)\frac{3a_{30}}{2\omega_3} + \frac{2c_2\eta_9\omega_2 a_{20}}{a_{30}\omega_3}\sin(\theta_{30}) + \frac{a_{30}\eta_{10}}{a_{20}}\cos(\theta_{30}) - \frac{a_{30}\eta_{11}}{a_{20}}\sin(\theta_{30})\right]a_{31} + \left[\frac{2c_2\eta_9\omega_2 a_{20}}{\omega_3}\cos(\theta_{30}) - \frac{\eta_{10}a_{30}^2}{2a_{20}}\sin(\theta_{30}) - \frac{\eta_{11}a_{30}^2}{2a_{20}}\cos(\theta_{30})\right]\theta_{31} - \left[\frac{\eta_1}{2\omega_2}a_{10}\right]a_{11} + \left[-\frac{\sigma_2}{a_{20}} + \frac{2\eta_{12}}{a_{20}} - \frac{\eta_1 a_{10}^2}{4\omega_2 a_{20}} - \frac{3a_{20}\eta_3}{4\omega_2} - \frac{f_{21}}{2a_{20}\omega_2}\cos(\theta_{20}) + \frac{2c_2\eta_9\omega_2}{\omega_3}\sin(\theta_{30})\right]a_{21} + \left[\frac{f_{21}}{2\omega_2}\sin(\theta_{20})\right]\theta_{21}. \tag{26b}$$

The eigenvalues of the above system of equations are given by the equation

$$\lambda^6 + r_1\lambda^5 + r_2\lambda^4 + r_3\lambda^3 + r_4\lambda^2 + r_5\lambda + r_6 = 0, \tag{27}$$

where $(r_1, r_2, r_3, r_4, r_5, r_6)$ are functions of the parameters $(a_1, a_2, a_3, \omega_1, \omega_2, \omega_3, \sigma_1, \sigma_2, \sigma_3, c_1, c_2, c_3, c_4, \beta_1, \beta_2, \beta_3, \beta_4, \beta_5, f_{12}, f_{21}, \alpha_1, \alpha_2, \theta_1, \theta_2, \theta_3)$. If the real part of the eigenvalue is negative, then the periodic solution is stable; otherwise, it is unstable. According to the Routh–Huriwitz criterion, the necessary and sufficient conditions for all the roots of (27) to have negative real parts is if and only if the determinant D and all its principle minors are positive:

$$D = \begin{vmatrix} r_1 & 1 & 0 & 0 & 0 & 0 \\ r_3 & r_2 & r_1 & 1 & 0 & 0 \\ r_5 & r_4 & r_3 & r_2 & r_1 & 1 \\ 0 & r_6 & r_5 & r_4 & r_3 & r_2 \\ 0 & 0 & 0 & r_6 & r_5 & r_4 \\ 0 & 0 & 0 & 0 & 0 & r_6 \end{vmatrix}. \tag{28}$$

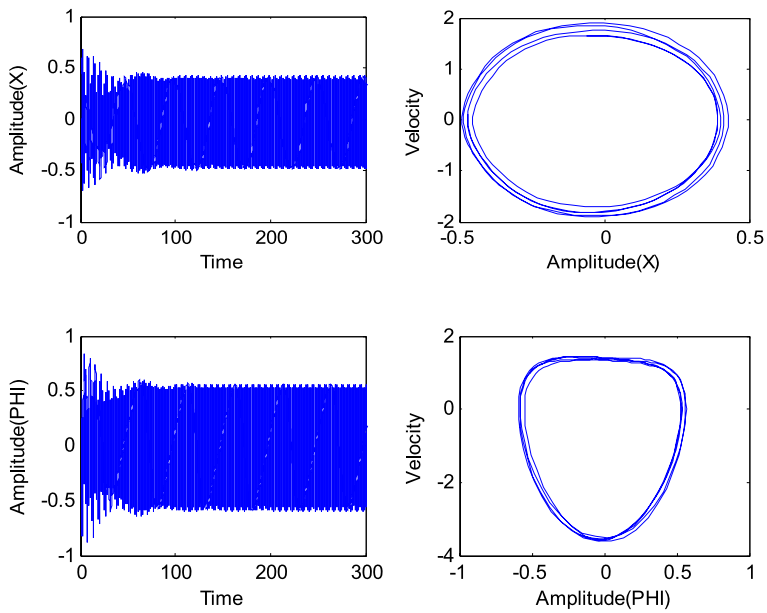

Fig. 2 Response of the system without absorber at simultaneous sub-harmonic resonance case ($\Omega_{12} \cong 2\omega_1$, $\Omega_{21} \cong 2\omega_2$)

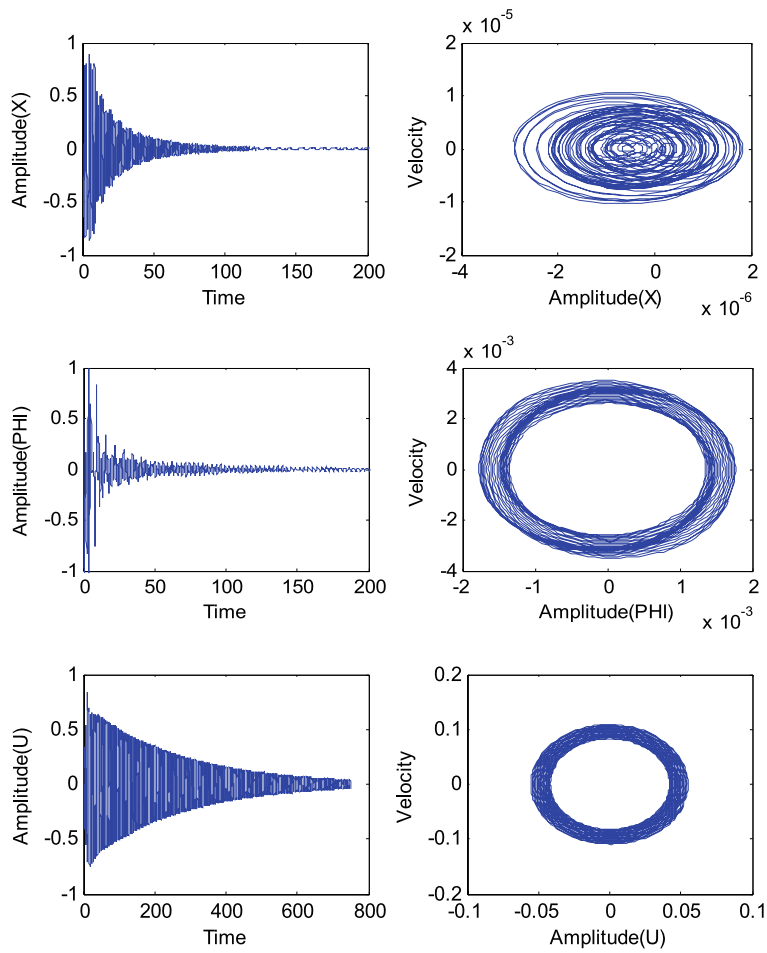

Fig. 3 Response of the system with absorber in simultaneous sub-harmonic and internal resonance case ($\Omega_{12} \cong 2\omega_1$, $\Omega_{21} \cong 2\omega_2$, $\omega_2 \cong 2\omega_3$)

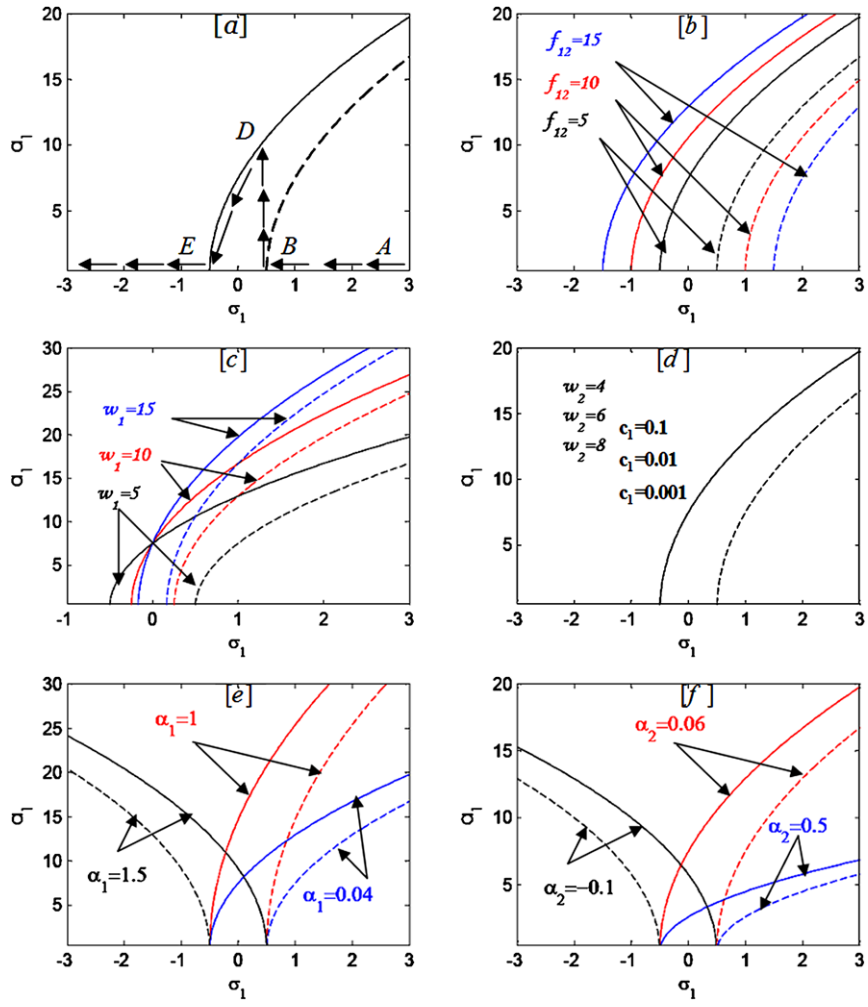

Fig. 4 Frequency response curves at selected values $\omega_1 = 5$, $\omega_2 = 4$, $c_1 = 0.01$, $a_1 = 0.01$, $f_{12} = 5$, $\alpha_1 = 0.04$, $\alpha_2 = 0.06$ and effect of different parameters

4 Results and discussion

In this section, (1)–(3) are numerically integrated using a fourth-order Rung–Kutta algorithm (via MATLAB 7.0). The numerical solutions of the spring pendulum with and without absorbers at simultaneous sub-harmonic and internal resonance are obtained as shown in Figs. 2 and 3 for the selected values ($\omega_1 = 5$, $\omega_2 = 4$, $\Omega_{12} \cong 2\omega_1$, $\Omega_{21} \cong 2\omega_2$, $\omega_2 \cong 2\omega_3$, $c_1 = 0.08$, $c_2 = 0.03$, $c_3 = 0.0008$, $c_4 = 0.008$, $\beta_1 = 0.4$, $\beta_2 = 0.03$, $\beta_3 = 0.06$, $\beta_4 = 0.3$, $\beta_5 = 0.6$, $\alpha_1 = 0.004$, $\alpha_2 = 0.006$, $f_{12} = 0.5$, $f_{21} = 0.4$).

In Fig. 2, the steady-state amplitude of the first mode (x) is about 80% of the first excitation force amplitude (f_{12}) and the steady-state amplitude of the second mode (φ) is about 150% of the second excitation force amplitude (f_{21}). The system of the both modes is stable with slight chaotic limit cycle, as shown in the phase plane trajectories.

Figure 3 illustrates the results at simultaneous sub-harmonic resonance when the absorber is effective, i.e., when $\Omega_{12} \cong 2\omega_1$, $\Omega_{21} \cong 2\omega_2$ and $\omega_2 \cong 2\omega_3$. It is clear from the figure that for the main system the steady-state amplitude of the first mode (x) and the second mode (φ) is reduced to 0.06% and 0.25% of the excitation forces amplitude (f_{12}, f_{21}), respectively, and the steady-state amplitude of the absorber (u) is about 0.04. This means that the effectiveness of the absorber E_a (E_a = steady-state amplitude of the main system without absorber/steady-state amplitude of the main system with absorber) is about 1300 for (x) and about 600 for (φ).

The frequency response equations are algebraic equations, which are solved numerically and the re-

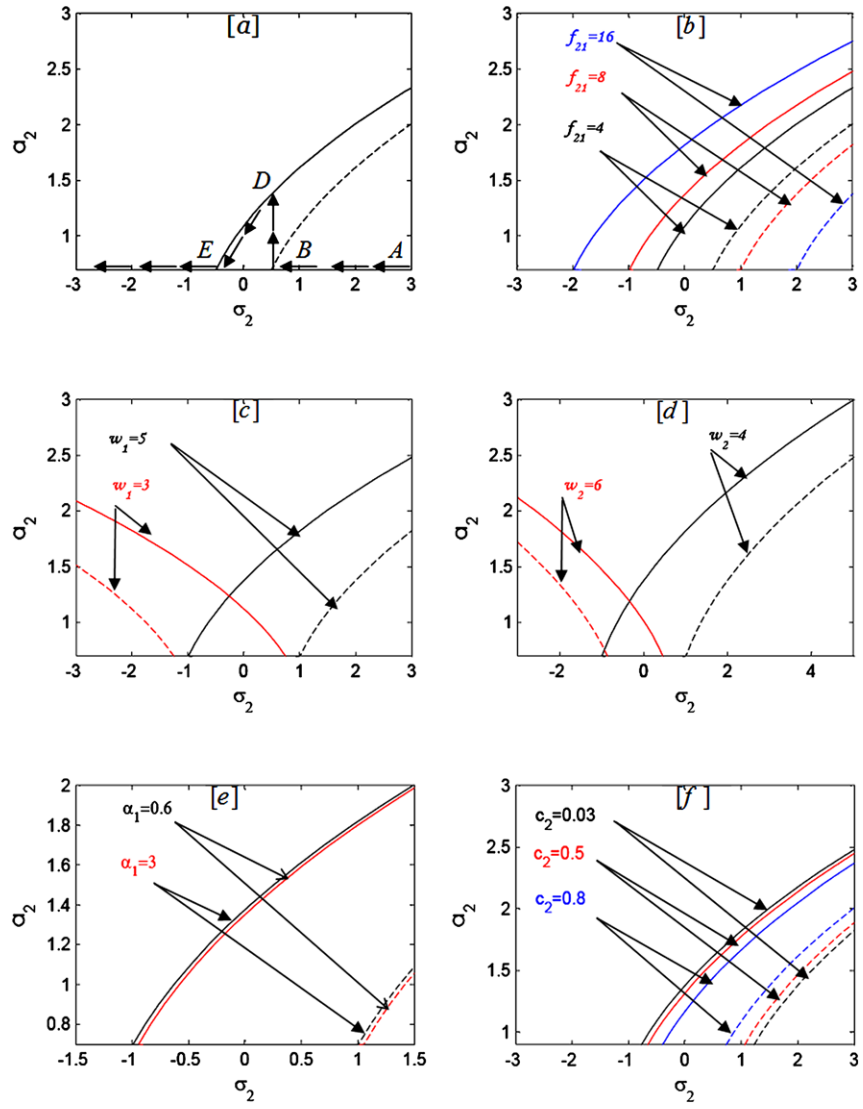

Fig. 5 Frequency response curves at selected values $c_2 = 0.03$, $\omega_1 = 5$, $\omega_2 = 2$, $\omega_3 = 4$, $\beta_1 = 0.4$, $\beta_2 = 0.03$, $\beta_4 = 0.3$, $\alpha_1 = 0.6$, $f_{21} = 8$, $\sigma_3 = 0.05$, $a_1 = 0.5$, $a_3 = 0.1$ and effect of different parameters

sults are presented in Figs. 4, 5 and 6, with (a_1, σ_1), (a_2, σ_2) and (a_3, σ_3) at selected values of some parameters.

Form the stability study of practical case ($a_1 \neq 0, a_2 \neq 0, a_3 \neq 0$) we can get the effect of the detuning parameter σ_1 on the steady-state amplitude a_1 of the first mode, as shown in Fig. 4(a). The curves consist of two branches: the solid line represents the stable solution while the dashed line represents the unstable solution, and accordingly their multi-valued solutions. Figure 4(b) shows that the steady-state amplitude is a monotonic increasing function of excitation amplitude f_{12}, which increases in unstable regions. From Fig. 4(c) we see that the steady-state amplitude is a monotonic decreasing function in ω_1 and the curve bends to right when ω_1 is decreased, which leads to the occurrence of jump phenomenon. Also, Fig. 4(d) shows that the effect of increasing or decreasing of the damping coefficient c_1 and ω_2 is trivial due to the occurrence of saturation. Figure 4(e) shows that increase or decrease of α_1 produces either soft or hard spring, respectively, and leads to occurrence of jump phenomenon. Increase or decrease of the value α_2 produces either hard or soft spring, respectively, and leads to the occurrence of jump phenomenon, as shown in Fig. 4(f).

We explain the jump phenomenon for example in Fig. 4(a). As σ_1 is reduced from a value correspond-

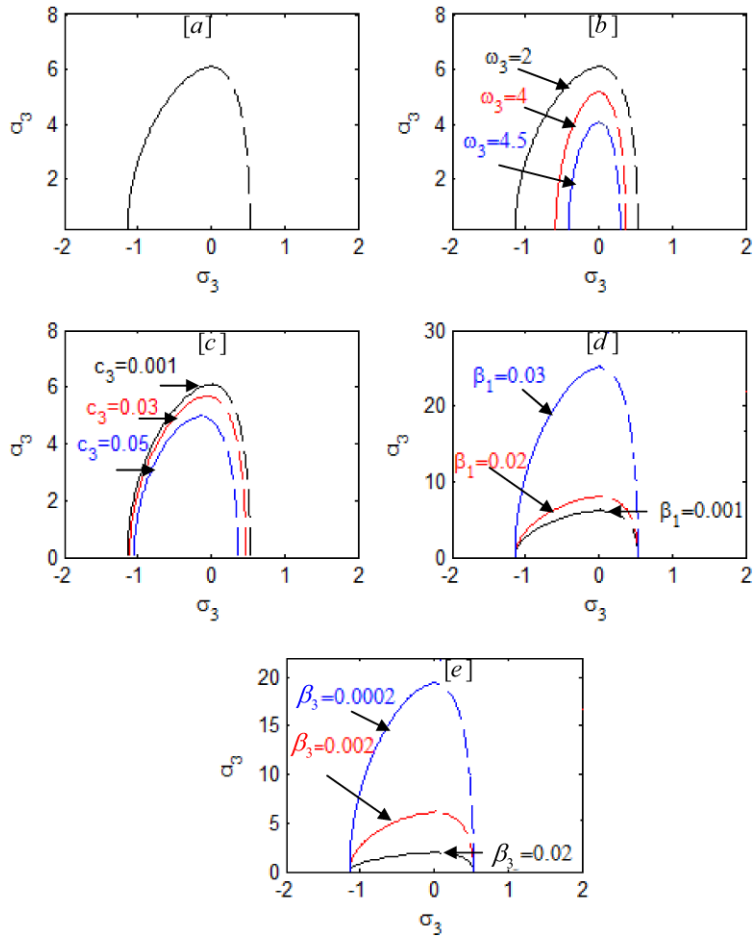

Fig. 6 Frequency response curves at selected values $c_2 = 0.03$, $\omega_1 = 10$, $\omega_2 = 2$, $\omega_3 = 4$, $\beta_1 = 0.4$, $\beta_2 = 0.001$, $\beta_3 = 0.002$, $\beta_4 = 0.01$, $\beta_4 = 0.02$, $\sigma_2 = 1$, $a_2 = 0.1$ and effect of different parameters

ing to the point A, the amplitude remains zero until the point B is reached. As σ_1 is decreased further, a jump takes place from the point B to the point D. Then, as σ_1 is decreased further, the amplitude decreases slowly. Also, we note that the region between B and E represents unstable trivial solutions; while for the other regions we have stable trivial solutions.

Figure 5(a, b, d) shows the effect of the detuning parameter σ_2 on the steady-state amplitude a_2. It shows that the effect of parameters (f_{21}, ω_2) of the amplitude (a_2) against the detuning parameter (σ_2) is similar to the effect of parameters (f_{12}, ω_1) of the amplitude (a_1) against the detuning parameter (σ_1) from Fig. 4. It can be seen from Fig. 5(c, e) that the increase of parameter ω_1, α_1 on the amplitude (a_2) is shifted and bent to right. Finally, Fig. 5(f) shows that the steady-state amplitude and the unstable region are monotonic decreasing functions of c_2.

The jump phenomenon in Fig. 5(a) is the same as one in Fig. 4(a).

Figure 6(a) shows the effect of the detuning parameter σ_3 on the steady-state amplitude a_3. Also, Fig. 6(b, c, e) shows that the steady-state amplitudes and the unstable region are monotonic decreasing functions in ω_3, c_3, β_3 and monotonic increasing functions in c_3 (see Fig. 6(d)). The effect of increasing or decreasing the damping coefficient c_2 and ω_1 is trivial due to the occurrence of saturation β_3.

5 Comparison with published works

(a) Literature review [5–8] studied a harmonically excited spring–pendulum system without any absorber while [14] studied the spring–pendulum system with transverse absorber but limited to a single external force only for each mode at primary and internal resonance case $(E_a(\varphi) = 15)$

and [25] studied the system with a longitudinal absorber where each mode is subjected to multi-parametric forces at sub-harmonic and internal resonance case ($E_a(x) = 6700$, $E_a(\varphi) = 120$).

(b) This paper illustrates the response of the two modes (x, φ) of the nonlinear spring–pendulum system when connected to transverse absorber subjected to multi-parametric excitations. We succeeded to reduce the steady-state amplitude of the first mode (x) to 0.08% and the second mode (φ) to 0.2% of its maximum value of the system without absorber via passive control method. This means that E_a of the first mode is approximately 1300 and 600 of the second mode at the simultaneous sub-harmonic and internal resonance case. Moreover, numerically the stable and unstable regions are defined when studying the effects of the selected parameters. It is worth to mention that a good agreement for reducing the vibration of the second mode (φ) of the system when we used the transverse absorber, more than if longitudinal absorber were used.

6 Conclusions

The vibration of a three-degree-of-freedom nonlinear spring pendulum which simulates the ship's roll motion subjected to multi-parametric excitation forces can be reduced (controlled passively) using a nonlinear tuned absorber which moves in the transverse direction. MSPT is applied to determine approximate solutions of the coupled nonlinear differential equations up to the second-order approximations near simultaneous sub-harmonic and internal resonance. Frequency response equations are deduced to investigate the system's stability. For the specific parameter values used in this paper the steady-state amplitude of the main system (x, φ) is reduced to 0.08% and 0.2%, respectively, of its original value. This means that the absorber effectiveness is about $E_a(x) = 1300$ and $E_a(\varphi) = 600$. Also, the unstable regions of the main system are decreasing when the values of f_{12} and f_{21} are decreasing and when the values of $c_2, \omega_1, \omega_2, \omega_3$ are increasing. Increase or decrease of both α_1 or α_2 produces either hard or soft spring, respectively, and leads to the occurrence of jump phenomenon.

Appendix

$$\eta_1 = \left(1 + \frac{7\omega_2^2 - 4\omega_1^2}{\omega_1^2 - 4\omega_2^2} - \frac{\alpha_1}{\omega_1^2}\right)2\omega_2^2,$$

$$\eta_2 = \left(\frac{10\alpha_1^2}{3\omega_1^2} - 3\alpha_2\right),$$

$$\eta_3 = \left(\frac{7\omega_2^2\omega_1^2 - 8\omega_2^4 + \omega_1^4}{2\omega_1^2(\omega_1^2 - 4\omega_2^2)}\right)\omega_2^2,$$

$$\eta_4 = \left(\frac{2\hat{c}_3\omega_2^2 - 2i\hat{\beta}_1\omega_2}{\omega_3^2 - \omega_2^2} - \hat{c}_2\right),$$

$$\eta_5 = \left[\left(\frac{2i\omega_3\beta_2\hat{c}_3 + 2\beta_2\hat{\beta}_1}{\omega_2^2 - \omega_3^2} - \frac{2i\hat{c}_3(\beta_2 - \beta_4)}{3\omega_3} - \frac{\hat{\beta}_1(\beta_2 - \beta_4)}{3\omega_3^2}\right)\right],$$

$$\eta_6 = \left[2i\omega_3\left(\frac{i\omega_3\hat{c}_3 + \hat{\beta}_1}{\omega_2^2 - \omega_3^2}\right) - \hat{c}_3 - \hat{c}_4\right],$$

$$\eta_7 = \left[\frac{10}{3\omega_3^2}\beta_2^2 - \frac{20}{3\omega_3^2}\beta_2\beta_4 + \frac{10}{3\omega_3^2}\beta_4^2 - 3(\beta_3 + \beta_5)\right],$$

$$\eta_8 = \left[\left(i\omega_3\hat{c}_2 + i\omega_3\hat{c}_3 + i\omega_3\hat{c}_4 + \hat{\beta}_1\right)\left(\frac{i\omega_3\hat{c}_3 + \hat{\beta}_1}{\omega_2^2 - \omega_3^2}\right)\right],$$

$$\eta_9 = \left[\frac{\beta_4}{\omega_3^2 - \omega_2^2} + \frac{\beta_2}{(\omega_2^2 - (\omega_2 - \omega_3)^2)}\right],$$

$$\eta_{10} = \left[\frac{\beta_2}{\omega_2} + \left(\frac{-\beta_2\beta_1}{\omega_2(\omega_2^2 - \omega_3^2)} + \frac{\beta_1(\beta_2 - \beta_4)}{3\omega_2\omega_3^2}\right) + \left(\frac{\sigma_3\beta_2}{2\omega_2^2} - \frac{\beta_1\beta_2}{2\omega_2^2\omega_3}\right)\right]$$

$$\eta_{11} = \left[\left(\frac{(2\omega_3 - \omega_2)\beta_2 c_3}{\omega_2(\omega_2^2 - \omega_3^2)} - \frac{2c_3(\beta_2 - \beta_4)}{3\omega_2\omega_3}\right) + \left(-\frac{c_2\beta_2}{4\omega_2^2} + \frac{c_4\beta_2}{2\omega_2^2} + \frac{c_3\beta_2}{2\omega_2^2}\right)\right],$$

$$\eta_{12} = \left(\frac{c_2c_3\omega_2}{2(\omega_3^2 - \omega_2^2)} - \frac{c_2^2}{4\omega_2} + \frac{c_2^2}{8\omega_2}\right),$$

$$\eta_{13} = \left[\frac{(c_3c_2\omega_3)}{2(\omega_2^2 - \omega_3^2)} + \left(-\frac{c_3^2}{8\omega_3} - \frac{c_4^2}{8\omega_3} - \frac{c_4c_3}{4\omega_3} - \frac{\beta_1^2}{8\omega_3^3}\right) + \frac{\beta_1}{2\omega_3}\right].$$

References

1. Mwad, D.J.: Passive Vibration Control. Wiley, Chichester (1988)
2. Meirovitch, L.: Fundamental of Vibrations. McGraw-Hill, New York (2001)
3. Nayfeh, A.H., Mook, D.T., Marshell, A.R.: Nonlinear coupled of pitch and roll modes in ship motions. J. Hydronaut. **7**(4), 145–152 (1973)
4. Tondl, A., Nabergoj, R.: Dynamic absorbers for an externally excited pendulum. J. Sound Vib. **234**(4), 611–624 (2000)
5. Lee, W.K.: A global analysis of a forced spring–pendulum system. Ph.D. Dissertation, University of California, Berkeley (1988)
6. Lee, W.K., Hsu, C.S.: A global analysis of a harmonically excited spring–pendulum system with internal resonance. J. Sound Vib. **171**(3), 335–359 (1994)
7. Lee, W.K., Park, H.D.: Chaotic dynamics of a harmonically excited spring pendulum system with internal resonance. J. Non-linear Dyn. **14**, 211–229 (1997)
8. Lee, W.K., Park, H.D.: Second order approximation for chaotic responses of a harmonically excited spring–pendulum system. Int. J. Non-Linear Mech. **34**, 749–757 (1999)
9. Eissa, M.: Vibration control of non-linear mechanical system via a neutralizer. Electronic Bulletin No 16, Faculty of Electronic Engineering Menouf, Egypt, July (1999)
10. Eissa, M., EL-Serafi, S., EL-Sheikh, M., Sayed, M.: Stability and primary simultaneous resonance of harmonically excited non-linear spring–pendulum system. Appl. Math. Comput. **145**, 421–442 (2003)
11. Eissa, M., Sayed, M.: A comparison between active and passive vibration control of non-linear simple pendulum, Part I: Transversally tuned absorber and negative $G\dot{\varphi}^n$ feedback. Math. Comput. Appl. **11**(2), 137–149 (2006)
12. Eissa, M., Sayed, M.: A comparison between active and passive vibration control of non-linear simple pendulum, Part II: Longitudinal tuned absorber and negative $G\ddot{\varphi}$ and $G\varphi^n$ feedback. Math. Comput. Appl. **11**(2), 151–162 (2006)
13. Sayed, M.: Improving the mathematical solutions of non-linear differential equations using different control methods. Ph.D. Thesis, Department of Mathematics, Faculty of Science, Menoufia, Egypt (2006)
14. Eissa, M., Sayed, M.: Vibration reduction of a three-DOF non-linear spring pendulum. Commun. Nonlinear Sci. Numer. Simul. **13**, 465–488 (2008)
15. Ayaz, Z., Vassalos, D., Turan, O.: Parametrical studies of a new numerical model for controlled ship motions in extreme astern seas. J. Marine Sci. Technol. **11**, 19–38 (2006)
16. Lee, D., Hong, S.Y., Lee, G.J.: Theoretical and experimental study on dynamic behavior of a damaged ship in waves. Ocean Eng. **34**, 21–31 (2007)
17. Bayly, P.V., Virgin, L.N.: An empirical study of the stability of periodic motion in the forced spring–pendulum. Proc. R. Soc. Lond. A **443**, 391–408 (1993)
18. Kamel, M.M.: Bifurcation analysis of a nonlinear coupled pitch–roll ship. Math. Comput. Simul. **73**, 300–308 (2007)
19. Zhou, L., Chen, F.: Stability and bifurcation analysis for a model of a nonlinear coupled pitch–roll ship. Math. Comput. Simul. **79**, 149–166 (2008)
20. Song, Y., Sato, H., Iwata, Y., Komatsuzaki, T.: The response of a dynamic vibration absorber system with a parametrically excited pendulum. J. Sound Vib. **259**(4), 747–759 (2003)
21. Amer, T.S., Bek, M.A.: Chaotic responses of a harmonically excited spring pendulum moving in circular path. J. Nonlinear Anal. **10**, 3196–3202 (2009)
22. Alasty, A., Shabani, R.: Chaotic motions and fractal basin boundaries in spring–pendulum system. J. Nonlinear Anal. **7**, 81–95 (2006)
23. Vyas, A., Bajaj, K.: Dynamics of auto-parametric vibration absorbers using multiple pendulums. J. Sound Vib. **246**(1), 115–135 (2001)
24. Osama, A.M., Nayfeh, A.H.: Control of ship roll using passive and active anti-roll tanks. Ocean Eng. **36**, 661–671 (2009)
25. Kamel, M., Eissa, M., EL-Sayed, A.T.: Vibration reduction of a non-linear spring pendulum under multi-parametric excitations via a longitudinal absorber. Phys. Scr. **80**, 025005 (2009) (12 pp.)
26. Nayfeh, A.H.: Perturbation Methods. Wiley, New York (1973)